

# **Preparation and characterization of an activated carbon based on coconut shell for the elimination of 2,4-dichlorophenoxyacetic acid in aqueous medium**

## **Abstract**

The objective of this work is to evaluate the capacity of activated carbon prepared from coconut shells to eliminate 2,4-dichlorophenoxyacetic acid. The characterization tests revealed that the specific surface area determined by the BET method is 570 m<sup>2</sup>/g consisting essentially of micropores. The chemical characteristics determined by the Boehm method indicate the acidic character of the carbon. The 2,4-dichlorophenoxyacetic acid adsorption tests revealed that the adsorption rate of 2,4-dichlorophenoxyacetic acid increases with increasing contact time, but decreases with increasing initial concentration. The adsorption capacity studied showed that the adsorption process of 2,4-D on activated carbon is controlled by pseudo-second order kinetics.

**Key words:** 2,4-dichlorophenoxyacetic acid, coconut shells, activated carbon, adsorption kinetics, phosphoric acid

## **1. Introduction**

The use of pesticides in modern agriculture is essential to maintain a level of production compatible with demand and needs. However, most of these molecules are highly toxic and difficult to biodegrade. Their massive and repeated use can have harmful consequences for all components of the environment [1]. 2,4-dichlorophenoxyacetic acid (2,4-D), an anionic herbicide, is widely used for weed control. [2]. However, it is considered moderately toxic and potentially carcinogenic [3]. Due to its low pK<sub>a</sub> value (2.73), it exists mainly in an anionic form, which can negatively affect aquatic life and the ecosystem. Moreover, its low biodegradability makes it an ecologically stable molecule [4]. The effects of this substance on surface or underground waters constitute an

environmental problem that requires decisions to be taken in order to overcome this degradation of the quality of our environment. Many techniques (biological, physical, and chemical) have been developed for their reduction or elimination in the environment [5]. However, most of these techniques turn out to be ineffective or too expensive. Nevertheless, adsorption, one of the most used techniques because of its ease of implementation and simplicity, is promising. Indeed, huge quantities of waste are generally available at the level of farms and agro-industrial facilities in many countries such as Côte d'Ivoire, where agricultural residues, in particular, represent a significant part. This study concerns the preparation and characterization of an activated carbon based on coconut shells for the elimination of 2,4-dichlorophenoxyacetic acid. The objective of this study is to enhance the quality of the activated carbon prepared and its effectiveness to remove 2,4-dichlorophenoxyacetic acid.

## **2. Materials and Methods**

### **2.1. Reagents and Solvents**

Carbon characterization tests have involved the use of various reagents and solvents. These included hydrochloric acid (HCl) with a concentration of 0.1 N, sodium thiosulfate ( $\text{Na}_2\text{S}_2\text{O}_3$ ) with 100% purity, sodium hydroxide (NaOH) with a purity of 99.9%, sodium carbonate ( $\text{Na}_2\text{CO}_3$ ) with a purity of 99 %, sodium hydrogen carbonate ( $\text{NaHCO}_3$ ) with a purity of 99 %, and orthophosphoric acid ( $\text{H}_3\text{PO}_4$ ) with a purity of 85%. Specifically, orthophosphoric acid has been used for impregnation during the chemical activation process.

### **2.2. Preparation of Activated Carbon**

The preparation of activated carbons was carried out following a previously described experimental plan [6]. The procedure involved several steps. Initially, the starting material, coconut shell, was washed with tap water to remove impurities. The washed material was then dried in an oven at 110 °C for a duration of 3 days. Once dry, the material was ground using a grinder and sieved to achieve a homogeneous particle size. The crushed material was subsequently impregnated in a solution of phosphoric acid ( $\text{H}_3\text{PO}_4$ ) for 24 hours.

After impregnation, the material was again dried in an oven at 110 °C until the complete evaporation of the impregnation liquid. Next, the dried samples were placed in crucibles and subjected to carbonization at a temperature of 600 °C for 4 hours. Following carbonization, the samples were thoroughly washed with distilled water while stirring, ensuring the pH of the rinsing water fell within the range of 6.5 to 7. Finally, the washed samples were dried once more in an oven at 110 °C for 24 hours and carefully packaged in ready-to-use glass jars.

### **2.3. Characterization of Activated Carbon**

#### **2.3.1. Iodine Number**

The iodine number was determined according to the experimental protocol [7] outlined below. In a 100 mL beaker, approximately 0.2 g of charcoal, previously dried in an oven at 110 °C for 24 hours, was taken. Using a pipette, 20 mL of the 0.02 N iodine solution was added to the beaker, and the mixture was stirred for 5 minutes. The resulting mixture was then filtered using ashless filter paper, and 10 mL of the filtrate was transferred to an Erlenmeyer flask. To determine the iodine number, sodium thiosulfate with a concentration of 0.02 mol/L was gradually added from a burette into the Erlenmeyer flask containing the filtrate until the solution completely lost its color. The volume of thiosulfate solution ( $V_{thio}$ ) in milliliters required for complete discoloration was recorded.

The iodine number expressed in mg/g is given by the following Equation. 1:

$$\text{Iodine number} \quad (1)$$

with:

$C_0$ : initial concentration of the iodine solution (mol/L)

$C_n$ : concentration of the sodium thiosulfate solution (mol/L),

$V_n$ : volume of sodium thiosulfate solution at equilibrium (mL),

$V_{I_2}$ : volume of the dosed iodine solution (mL),

$V_{ads}$ : adsorption volume (mL),

$M_{I_2}$ : molar mass of iodine (g/mol),

$m_{CA}$ : mass of activated carbon (g).

### 2.3.2. Surface functions

The measurements are carried out according to the [8] as follows: 1 g of dry activated carbon is brought into contact with 50 mL of each of the 0.1 N aqueous solutions of NaOH, Na<sub>2</sub>CO<sub>3</sub>, NaHCO<sub>3</sub>, and HCl. Each solution is stirred for 24 hours to ensure that as many surface groups of the activated carbon have reacted as possible. After filtration, an acid-base assay is conducted on 10 mL of each solution. The basic solutions are titrated with 0.1 M hydrochloric acid, and the acid solution is titrated with 0.1 N sodium hydroxide

### 2.3.3. Zero charge pH (pHpzc)

The determination of pHpzc (Point of zero charge) was carried out using the following procedure: Initially, 50 mL of distilled water was placed in sealed bottles, and the pH of each solution was adjusted within the range of 2 to 12 by adding either NaOH or HCl solution (0.1 M). Subsequently, 0.5 g of the sample material to be characterized was added to each bottle. The suspensions were stirred continuously at room temperature for 24 hours, after which the final pH was measured. By plotting  $\Delta\text{pH} = f(\text{pH}_i)$  on a graph, where  $\Delta\text{pH}$  represents the difference between the final pH (pH<sub>f</sub>) and the initial pH (pH<sub>i</sub>), the isoelectric point was determined by identifying the intersection of the curve with the bisector of the ordinate and abscissa axis.

### 2.3.4. Specific surface

The determination of the BET specific surface area of an activated carbon is performed using the Brunauer-Emmett-Teller (BET) method. This method relies on measuring the quantity of nitrogen adsorbed by the activated carbon. The BET equation, derived from the assumptions of the BET theory for gas adsorption on a solid, enables the calculation of the specific surface area of the analyzed sample. The equation 2 used for this calculation is as follows:

$$(2)$$

where Q and Q<sub>m</sub> represent respectively the quantity of gas adsorbed at the pressure P and the quantity of gas necessary for the covering of 1g of adsorbent with a single layer of gas.

C is the BET constant.

The plot of the curve as a function of  $P/P_0$  gives an affine straight line with equation  $y = ax + b$ , with slope and with y-intercept . We deduce from this equation 3 the terms  $Q_m$  and C as follows:

$$\text{et} \tag{3}$$

From these parameters, the specific surface of the adsorbent is determined according to the following equation. 4:

$$\tag{4}$$

where  $\sigma$  is the area occupied by an adsorbate molecule ( $0.162 \text{ nm}^2$ ) and N is Avogadro's number ( $6.02 \cdot 10^{23} \text{ mol}^{-1}$ ).

### 2.3.5. t-plot method

The t-plot method, in conjunction with the BET surface analysis, was employed to determine the porous surface value of the carbon [9]. By considering the number of molecular layers adsorbed at a specific pressure (P) on the solid, which is obtained by dividing the volume of vapor adsorbed at each pressure (V) by the calculated monolayer volume ( $V_m$ ) derived from the BET equation, the thickness (t) was determined. The statistical thickness of a monomolecular layer (e) was used in the calculation, and the relationship between these variables can be expressed in equation 5:

$$\tag{5}$$

### 2.3.6. Imaging of the porous surface of coal

The scanning electron microscope (SEM) is a technique that utilizes electron-matter interactions to generate high-resolution images of a sample's surface [10]. In this study, the analysis was conducted at the Analysis and Research Center of PETROCI in Abidjan, Côte d'Ivoire. The specific equipment used for the SEM analysis was the FEG Supra VP Zeiss model.

An electron beam is directed towards the sample under analysis. The interaction between the electron beam and the sample results in the generation of low-energy secondary

electrons, which are then accelerated towards a secondary electron detector to amplify the signal. At each point of impact, an electronic signal is produced, providing information about the composition and characteristics of the sample at that specific location. By scanning the sample with the electron beam, it is possible to create a comprehensive map of the sample, revealing its features and properties. The three-dimensional image appears on the phosphor screen and can be saved. The metallized sample is analyzed using a scanning electron microscope (SEM) coupled with energy dispersive spectroscopy (EDS). This gives the elemental composition and topography of the ports.

## **2.4 Adsorption tests**

### **2.4.1. Effect of contact time**

To demonstrate the effect of contact time on adsorption kinetics, a 0.5g gram mass of activated carbon is brought into contact with 50 mL of the pollutant (2,4-D) at a concentration of 5 mg/L in an Erlenmeyer flask. The mixture is stirred using a magnetic stirrer at a temperature of 25 degrees Celsius and a speed of 150 rpm for times ranging from 5min to 180 min. The suspension obtained after the stirring time is centrifuged, then filtered, and analyzed with an UV-Vis spectrophotometer to determine the residual concentration of 2,4-D.

### **2.4.2. Effect of mass of activated carbon**

In this test, different masses of adsorbent were taken (0.1 g, 0.25 g, 0.5 g, 0.75 g, and 1.25 g). Each mass of adsorbent was brought into contact with 50 mL of a 2,4-D solution at a concentration of 5 mg/L in an Erlenmeyer flask. For each mass of activated carbon, the mixture was stirred using a magnetic stirrer at a speed of 150 rpm for the predetermined reaction time (Tr). The suspension obtained was centrifuged and filtered before analysis to determine the residual concentrations using an UV-Vis spectrophotometer.

### **2.4.3. Effect of initial 2,4-D concentration**

The effect of 2,4-D concentration on adsorption was determined by bringing the dose of adsorbent obtained previously into contact with different concentrations of 2,4-D, ranging from 0.5 mg/L to 15 mg/L, in an Erlenmeyer flask. For each concentration of 2,4-D, the

mixture was stirred using a magnetic stirrer at a speed of 150 rpm for the equilibrium time obtained previously. The suspension obtained after centrifugation was filtered and analyzed to determine the residual concentration using an UV-Vis spectrophotometer.

### 3. Results and discussion

#### 3.1. Activated carbon characterization

##### 3.1.1. Iodine number

The iodine number is a fundamental parameter for characterizing the performance of activated carbons. It provides a good estimate of the total surface area available for the adsorption of low molecular weight compounds. The iodine index value for the activated carbon in this study is 446.706 mg/g. This value is similar to those reported by [11], who found iodine index values between 482 and 852 mg/g for *Zizyphus Mauritiana*, and by [12], who found an iodine index value of 550 mg/g for coconut husk.

##### 3.1.2. Surface chemistry

The determination of the surface functionalities by the Boehm titration method made it possible to determine the nature and quantities of the functional groups of the activated carbons (Table 1). It was noted that the activated carbon has an acidic character with the existence of basic groups on the surface of the carbon. This gives it a double efficiency vis-à-vis the chemical nature of the pollutant to be treated. These same observations were made by [13]. Their research was focused on the study of four activated carbons from coconut shells.

**Table 1:** Surface functions of prepared activated carbon (AC)

Chemical functions	Carboxylic function	Lactone function	Phenol function	Total acidity	Total basicity
AC	2.13	0.08	0.04	2.25	1.42

##### 3.1.3. pH point of zero charge (pHpzc)

The value of 4.01 (Figure 1) corresponds to the isoelectric point of the activated carbon obtained. This pHpzc value indicates the acidic nature of the activated carbon, which can

be attributed to the activating agent (phosphoric acid) and the composition of the initial biological material. The  $pH_{pzc}$  serves as an indicator of the adsorbent's behavior towards the adsorbate. If the solution's pH is lower than the  $pH_{pzc}$  ( $pH < 4.01$ ), the adsorbent will become protonated due to an excess of  $H^+$  protons from the solution's surface functional groups. This protonation makes the support material attractive to negatively charged adsorbates. Conversely, if the solution's pH is higher than the  $pH_{pzc}$ , the adsorbent will be deprotonated by the  $OH^-$  ions present in the solution's surface functional groups, causing the support to attract positively charged adsorbate [14].

**Fig. 1.** Determination of the pH point of zero charge ( $pH_{pzc}$ ) of the activated carbon

#### **3.1.4. Estimation of specific surface and porosity**

The results for the adsorption and desorption isotherms of nitrogen ( $N_2$ ) at 77 K are depicted in Figure 2A. This figure illustrates that the curve closely resembles a type I isotherm, as per the classification proposed by [15]. This type of isotherm is characteristic of a microporous adsorbent. It occurs when the concentration of the solution increases, leading to a decrease in available adsorption sites. [16] suggest that this phenomenon arises when the forces of attraction between the adsorbed molecules are weak. The adsorption isotherm allows access to the specific surface area. By utilizing the BET equation (Fig. 2B), a straight line is obtained, and the specific surfaces are calculated following the BET method. Nitrogen ( $N_2$ ) adsorption isotherms also provide information regarding the actual pore area, volume, and diameter. The pore size distribution is determined using the technique developed by [17].

Fig. 2. Adsorption and desorption isotherms of  $N_2$  on activated carbon (A) and straight line obtained from the BET equation (B)



Figure 3 shows the distribution of area and volume as a function of pore diameter. It reveals that the external surface accounts for approximately 98 % of the total surface area. The results obtained from the analysis of the curves are displayed in table 2. The examination of this table demonstrates that the activated carbon possesses a BET surface area of 570.761 m<sup>2</sup>/g, primarily dominated by micropores (506.78 m<sup>2</sup>/g or 88.79%). This could be attributed to the characteristics of the precursor material and the activating agent (phosphoric acid). As coconut shells are lignocellulosic materials, the use of phosphoric acid as an activating agent not only contributes to the creation of new pores but also to the enlargement of existing ones in the precursor [18]. Additionally, the dehydrating oxidizing agent H<sub>3</sub>PO<sub>4</sub> reacts within the internal structure of cellulose, resulting in depolymerization and an increase in total pore volume [19].

**Fig. 3** Distribution of surface area as a function of pore diameter (A) and pore volume as a function of pore diameter (B)

**Table 2 .** Porous properties of activated carbon

Total surface area SBET (m <sup>2</sup> /g)	BET	570.761
Area of the microporous surface (m <sup>2</sup> /g)	(t-plot)	506.780
External surface area Sext (m <sup>2</sup> /g)	(t-plot)	63.981
Microporous volume (cm <sup>3</sup> .g <sup>-1</sup> )	(t-plot)	0.0264

### 3.1.5. Imaging the Porous Surface of Coal

The figure 4 indicates the distribution of various pore sizes with open porosity. The presence of macropores and mesopores is more pronounced compared to micropores. The presence of macropores and mesopores is more pronounced than that of micropores suggests that, in the coals studied, the concentration or abundance of macropores and mesopores in the material examined is higher than that of micropores. Indeed, pores are empty spaces within a material and can be classified into different categories according to

their size. Micropores are the smallest, their diameter generally being less than 2 nm, while mesopores are larger, their diameter being between 2 and 50 nm, and macropores are the largest, their diameter generally being greater than 50 nm.

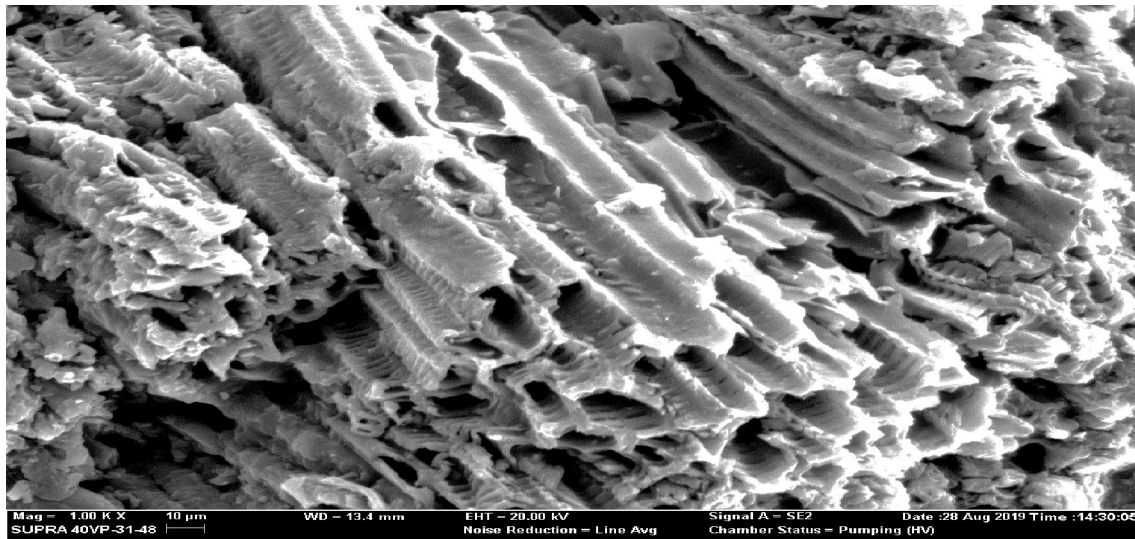


Fig. 4. Scanning Electron Microscope image of activated carbon (AC) pore topography

## 3.2 Adsorption Tests

### 3.2.1 Influence of Contact Time on Adsorption

Studying the influence of stirring time allows us to determine the time required to reach adsorption equilibrium. The results obtained, presented as the adsorption rate versus time, are shown in Figure 5. In this figure, we observe a rapid increase in the adsorption of 2,4-dichlorophenoxyacetic acid within the range of 0 to 40 min, with an adsorption rate ranging from 0% to 51.73%. This is followed by a slower adsorption phase from 40 to 100 min, with an adsorption rate between 51.73% and 67.73%. Beyond 100 min, the system reaches an equilibrium phase with a constant adsorption rate. This equilibrium time corresponds to the maximum efficiency of 2,4-D adsorption, after which the adsorption

rate no longer changes, resulting in a saturation plateau. The rapid adsorption rate observed in the initial phase can be attributed to the availability of free adsorption sites on the activated carbon. As the 2,4-D molecules occupy a majority of these sites, the adsorption rate gradually slows down (slow phase). When all the available adsorption sites are occupied by the 2,4-D molecules, the adsorption rate reaches a plateau (saturation phase). These findings align with those reported by [20].

Fig.5. Effect of contact time on 2,4-D adsorption

### **3.2.2 Effect of Activated Carbon Mass on 2,4-D Removal**

The results of the adsorption tests investigating the influence of the adsorbent mass are depicted in Figure 6. In this figure, a rapid increase in adsorption is observed as the mass of activated carbon varies from 0.1 g to 1.25 g. The adsorption rate for this range of mass change rises from 90.91 % to 96.93 %. Indeed, the adsorption rate increases with an increase in the mass of activated carbon. The adsorption rate of 2,4-D rises from 30.26% to 88.16% when the mass of activated carbon changes from 0.1 g to 1.25 g. This correlation between the adsorption rate and carbon mass can be explained by the fact that an increase in mass leads to a greater exchange surface area, specifically an increase in the availability of adsorption sites [21]. A mass of 0.5 g of activated carbon, resulting in an adsorption rate of 95.348%, was selected for subsequent adsorption tests.

Fig. 6. Effect of activated carbon mass on 2,4-D

### **3.2.3. Effect of Initial Solution pH on 2,4-D**

The influence of pH on adsorption was examined to determine the optimal pH for adsorption. The pH was varied from 2 to 11 for a mass of 0.5 g of activated carbon in contact with 50 ml of 2,4-D at a concentration of 5 mg/L and at the designated equilibrium time. The results, expressed as the adsorption rate as a function of pH, are presented in Figure 7. It is observed that the adsorption rate reaches its maximum values in an acidic environment (pH = 2) before gradually decreasing as the pH moves towards a

basic environment. When the pH increases from 2 to 11, the adsorption rate for carbon decreases from 85.5% to 17.1%. The pH of the 2,4-D solution has a significant impact on the adsorption capacity. As the pH increases, the degree of dissociation of 2,4-D acid increases, resulting in a negative charge on the molecule. Considering the low pKa of the 2,4-D molecule (2.73), it becomes negatively charged in its conjugate acid form. Moreover, the carbon surface exhibits positive charge in an acidic environment ( $\text{pH} < \text{pH}_{\text{pzc}}$ ), which promotes the attraction between the adsorbent and adsorbate [22].

Fig. 7. Effect of pH on 2,4-D adsorption

### 3.2.4 Influence of the Initial Concentration of 2,4-D

Analyzing the curve, it can be observed that the adsorption rate decreases as the concentration of 2,4-D increases (Figure 8). Specifically, when the concentration of 2,4-D increases from 5 mg/L to 30 mg/L, the adsorption rate decreases from 72.36 % to 44.08 %. The increase in initial concentration leads to a higher number of 2,4-D molecules, while the number of available adsorption sites remains constant. This phenomenon can be explained by the fact that the driving force for adsorption increases with higher concentration, facilitating the transfer of the solute from the solution to the sorbents [23].

Fig. 8. Effect of initial concentration of 2,4-D solution

### 3.2.5. Modeling of adsorption kinetics

The kinetics of cobalt adsorption are modeled using three models: the pseudo-second order kinetic model, pseudo-first order kinetic model, and the intraparticle diffusion model.

#### 3.3.1 Pseudo-First order kinetic model

The pseudo-first order model was investigated using the Lagergren equation 6:

$$\ln(Q_e - Q_t) = -kt + \ln Q_e$$

(6)

The relationship between  $\ln(Q_e - Q_t)$  and time ( $t$ ) is illustrated in Figure 9, allowing for the determination of the equilibrium adsorbed quantity of 2,4-D and the rate constant of the pseudo-first order model. The representations of  $\ln(Q_e - Q_t) = f(t)$  (Figure 35) are not linear lines, thus indicating the invalidity of the Lagergren equation for the description of the adsorption kinetics of 2,4-D by the CA. The results are reported in table 3.

Fig. 9. Pseudo-first order kinetics model of 2,4-D adsorption.

### 3.3.2 Pseudo-second order kinetic model

The plot of the curve  $t/Q_e$  as a function of time ( $t$ ) yields a straight line with a slope of  $1/Q_e$  and an ordinate at the origin of  $1/(k_2 * Q_e^2)$ , enabling the calculation of the rate constant of the surface adsorption reaction ( $k_2$ ) and the equilibrium adsorption amount ( $Q_e$ ) in mg/g (Figure 10). This representation in the form of a straight line suggests a good description of the 2,4-D adsorption process. The results are illustrated in table 3.

Fig.10: Pseudo-second-order kinetics model of 2,4-D adsorption

The results show that the calculated quantities of 2,4-D adsorbed ( $Q_{e,cal}$ ) using the pseudo-second-order model are comparable to the experimentally obtained values ( $Q_{e,exp}$ ). Additionally, the coefficient of determination ( $R^2 = 0.99$ ) for the pseudo-second-order model is close to unity, indicating a strong correlation between the experimental and theoretical data. In contrast, the pseudo-first-order models exhibit coefficients of determination that are far from unity. Therefore, the pseudo-second-order kinetic model provides the best description of the adsorption kinetics of 2,4-dichlorophenoxyacetic acid

on the studied activated carbon. These findings align with the results reported by [23] and [24] who also investigated the removal of 2,4-D using activated carbon.

**Table 3.** Kinetic models parameters for the adsorption of 2,4-D on activated carbon

Model	Parameters	Concentration of 2,4-D (mg/L)			
		5	10	15	30
Pseudo-first order	<b>R<sup>2</sup></b>	<b>0.979</b>	<b>0.995</b>	<b>0.942</b>	<b>0.977</b>
	K <sub>1</sub> (min <sup>-1</sup> )	-0.0746	-0.068	-0.067	1.336
	Q <sub>ecal</sub> (mg.g <sup>-1</sup> )	0.3174	0.596	0.629	0.134
	Q <sub>eexp</sub> (mg.g <sup>-1</sup> )	0.362	0.664	0.809	1.52
Pseudo-second order	<b>R<sup>2</sup></b>	<b>0.997</b>	<b>0.997</b>	<b>0.998</b>	<b>0.995</b>
	K <sub>2</sub>	0.1323	0.056	0.082	0.015
	Q <sub>ecal</sub> (mg.g <sup>-1</sup> )	0.4095	0.7699	0.8431	1.83
	Q <sub>eexp</sub> (mg.g <sup>-1</sup> )	0.362	0.664	0.809	1.52

### 3.2.6. Intra-particle diffusion model

Figure 11 presents the graphical results of this model. The differences obtained are recorded in table 3. This figure reveals three linear phases. This multilinear representation of intraparticle diffusion shows that the 2,4-D adsorption process is not controlled only by intraparticle diffusion [25]. Furthermore, the lines are not linear. On the other hand, the adsorption process of 2,4-D on CA could be controlled by external, internal diffusion and intra-particle diffusion.

Fig.11: Kinetic model according to intra-particle diffusion

## 4. Conclusion

This study focused on the kinetics of 2,4-D adsorption using activated carbon derived from coconut shells. The adsorption tests demonstrated that the adsorption capacity of 2,4-D decreases with an increase in the mass of carbon, with a maximum adsorption rate of 85.5% observed at pH 2 for a carbon mass of 0.5 g. Furthermore, the influence of 2,4-D concentration revealed a decrease in adsorption capacity as the concentration of 2,4-D increased. The investigation of the adsorption kinetics of 2,4-D indicated that the pseudo-second-order model provides a better description of the adsorption process compared to other models, as it exhibits a correlation coefficient close to unity ( $R^2 = 0.99$ ). Overall, this study highlights the potential of activated carbon derived from coconut shells as an effective adsorbent for 2,4-D removal. The findings contribute to a better understanding of the adsorption behavior and kinetics of 2,4-D on activated carbon, supporting its potential application in water treatment and environmental remediation processes.

## References

[1] Lanouari S., NasseB. r, El Haddoury J. & Bencharki B. (2015). Caractérisation physico-chimique des graines de blé tendre (*Triticum aestivum*) sous traitement herbicide

par l'acide 2,4-dichlorophénoxyacétique. *International Journal of Innovation and Applied Studies*, 10, 604-620.

[2] Salman J.M., Njoku V.O. & Hameed B.H. (2011). Adsorption of pesticides from aqueous solution onto banana activated carbon stalk. *Chemical Engineering Journal*, 10 (174): 41– 48.

[3] Chao Y.-F., Chen P.C. & Wang S.L.(2008). Adsorption of 2,4-D on Mg/Al-NO<sub>3</sub> layered double hydroxides with varying layer charge density. *Applied. Clay Science.*, 40193-200.

[4] Carter A.D. (2000). Herbicide movement in soils: principles, pathways and processes. *Weed Research.*, 40, 113-122 .

[5] Pokhe D. L & Viraraghavan T. (2004). Treatment of pulp and paper mill wastewater: a review, *Science of the Total Environment.*, 333, 37-58.

[6] Dibi K.; Méité L., Aboua K.N., Soro D.B, Konan G., Kossonou N.R., Traoré S.K & Mamadou K., (2021). Optimizing the preparation conditions of activated carbon from coconut shells using a full factorial design. *International Journal of Innovation and Applied Studies.*, 33, 214-22.

[7] Rager T., Geoffroy A., Hilfikera R., John M. & Storeyb D. (2012). The crystalline state of methylene blue: a zoo of hydrates. *Chimie- Physique.*, 14, 8074-8082.

[8] Boehm H. P. (1994). Chemical identification of surface groups. *Advance catalys*, vol. 16, 25-31.

[9] Lippens B.C. & De Boer J.H. (1965). Studies on Pore Systems in Catalysts. V. The *t* Method. *Journal of Catalysis*, 4, 319-323.

[10] Habeeb O.A., Yasin F.M. & Danhassan U.A. (2014). Characterization and application of chicken eggshell as green adsorbents for removal of H<sub>2</sub>S from wastewaters. *Journal. Environmental Sciences., Toxicology and Food Technology*, 8, 7-12.

[11] Mamane O.S., Adamou Z., Ibrahim D. & Ibrahim N. (2016). Préparation et caractérisation de charbon à base de coques de balanite Eagyptiaca et de Zizyphus Mauritania. *Journal de la Société Ouest-Africaine de Chimie*, 41, 59-67.

[12] Gueye M. (2015). Développement de charbon actif à partir de biomasses



lignocellulosiques pour des applications dans le traitement de l'eau. Thèse de doctorat de l'Institut International de l'Ingénierie de l'Eau et l'Environnement (2IE), Ouagadougou, Burkina Faso, 215p.

[13] Gbamélé K.S., Athéba G.P., Dongu B.K. i, Drogui P., Robert D., Kra O.D., Konan S., De Bouanzi G.G.M. & Trokouré A. (2016). Contribution à l'étude de quatre charbons activés à partir des coques de noix de coco. *Afrique Science*, 12, 229-245.

[14] Hamee B.H. (2009) "Evaluation of papaya seed as a novel non-conventional low-cost adsorbent for removal of methylene blue. *Journal Hazard. Mater.*, 162, 939-994.

[15] Giles C.H., Smith D. & Alan H. (1974). A general treatment and classification of the adsorption isotherm. *Journal of Colloid Interface Science*, (47), 755-765.

[16] Avom J., Ketcha M.J., Matip M.R.L. & Germain P. (2001). Adsorption isotherme de l'acide acétique par des charbons d'origine végétale. *African. Journal of Science and Technology, Science and Engineering*, 2, 1-7.

[17] Barrette E.P., Joyner L.G. & Halenda P.P. (1951). The determination of pore volume and area distributions in porous substances. I. Computations from Nitrogen isotherms. *Journal American. Chemical Society*, 73, 373-380.

[18] Sanogo D., Aboua K.N., Soro D.B., Méité L., Kouadio D.L., Diarra M., Ehouman A.G.S., Traoré K.S. & Dembélé A. (2020). Adsorption of l'acide Green 42 en solution aqueuse sur un charbon actif issu des coques des gousses de moringa. *Journal of Chemical, Biological and Physical Sciences*, 10, 211-220.

[19] Jagtoyen M. & Derbyshire F. (1998). Activated carbons from yellow poplar and white oak by  $H_3PO_4$  activation. *Carbon*, 36, 1085-1097.

[20] Youssef A.M., EL-Didamony H., EL-Sharabasy S.F., Sobhy M., Hassan A.F. & Buláneke R., (2017). Adsorption of 2, 4-dichlorophenoxyacetic acid on different types of activated carbons based date palm pits: kinetic and thermodynamic studies *International Research Journal of Pure & Applied Chemistry*, 14, 1-15.

[21] Boughaita I. (2018). Essais de dépollution des eaux contaminées par un composé organique par l'utilisation de nouveaux biosorbants. Thèse de Doctorat, Université 20 Août 1955-Skikda, République Algérienne Démocratique et Populaire, 103p.

[22] Hameed B.H., Salman J.M. & Njoku V.O., (2011). Batch and fixed-bed adsorption

of 2,4-dichlorophenoxyacetic acid onto oil palm frond activated carbon. *Chemical Engineering Journal*, 174, 33– 40 (8 pages)

[23] Jassem M.S., Abdulkarim M. & Huda S.H. (2011). Adsorption of 2,4-dichlorophenoxyacetic acid onto coconut activated carbon: kinetics and equilibrium studies. *Al-Mustansiriyah Journal of Science*, 22, 377-384.

[24] Dehghani M., Nasser S. I & Karamimanesh M. (2014). Removal of 2,4-Dichlorophenoxyacetic acid (2,4-D) herbicide in the aqueous phase using modified granular activated carbon. *Journal. Environmental. Health Science Engineering*, 12 (1):28

[25] Melouki S., (2021). Synthèse, caractérisation de charbons actifs fonctionnalisés et étude de leurs applications en élimination de polluants. Thèse de doctorat de l'Université Mohamed Boudiaf de M'sila, Algérie, p 115.